ANTIMICROBIAL AGENTS AND CHEMOTHERAPY, May 2002, p. 1253–1261 Vol. 46, No. 5
0066-4804/02/$04.00+0 DOI: 10.1128/AAC.46.5.1253–1261.2002

Identification of Essential Residues in the Erm(B) rRNA Methyltransferase of *Clostridium perfringens*

Kylie A. Farrow,[1] Dena Lyras,[1] Galina Polekhina,[2] Katerina Koutsis,[1] Michael W. Parker,[2] and Julian I. Rood[1]*

Bacterial Pathogenesis Research Group, Department of Microbiology, Monash University, Clayton, Victoria 3800,[1] *and Biota Structural Biology Laboratory, St. Vincent's Institute of Medical Research, and The University of Melbourne, Fitzroy, Victoria 3065,*[2] *Australia*

Received 20 September 2001/Returned for modification 29 November 2001/Accepted 24 January 2002

Macrolide-lincosamide-streptogramin B resistance is widespread, with the determinants encoding resistance to antibiotics such as erythromycin being detected in many bacterial pathogens. Resistance is most commonly mediated by the production of an Erm protein, a 23S rRNA methyltransferase. We have undertaken a mutational analysis of the Erm(B) protein from *Clostridium perfringens* with the objective of developing a greater understanding of the mechanism of action of this protein. A recombinant plasmid that carried the *erm*(B) gene was mutated by either in vitro hydroxylamine mutagenesis or passage through the mutator strain XL1-Red. Twenty-eight independently derived mutants were identified, nine of which had single point mutations in the *erm*(B) gene. These mutants produced stable but nonfunctional Erm(B) proteins, and all had amino acid changes within conserved methyltransferase motifs that were important for either substrate binding or catalysis. Modeling of the *C. perfringens* Erm(B) protein confirmed that the point mutations all involved residues important for the structure and/or function of this rRNA methyltransferase. These regions of the protein therefore represent potential targets for the rational development of methyltransferase inhibitors.

Macrolide, lincosamide, and streptogramin B (MLS) antibiotics are a diverse group of antibacterial agents that are chemically distinct but that have similar modes of action. They act at the early stages of protein synthesis by blocking the growth of the nascent peptide chain (1), which then presumably causes the premature dissociation of the peptidyl-tRNA molecule from the ribosome (22). These antibiotics include erythromycin, clindamycin, and lincomycin and are active against various bacteria, including gram-positive cocci and rods and gram-negative cocci.

Four mechanisms of bacterial resistance to MLS antibiotics have been detected; they involve enzymatic modification of the antibiotic, active efflux from the bacterial cell, mutation of the ribosomal target site, or, most commonly, enzyme-mediated chemical alteration of the rRNA target (18, 19, 33). The last mechanism is mediated by the synthesis of a 23S rRNA methyltransferase, which is responsible for the N^6-dimethylation of a specific adenine residue in the 23S rRNA molecule (17).

Methyltransferases are enzymes that methylate a wide variety of substrates; they use *S*-adenosyl-L-methionine (SAM) as the universal methyl donor and release *S*-adenosyl-L-homocysteine as the reaction product (4). Comparative analysis of over 40 DNA amino-methyltransferases (21) revealed the presence of nine conserved sequence motifs that are important in target sequence specificity, catalysis, and SAM binding (Fig. 1). Motif I is highly conserved and forms a secondary structure known as the G loop which binds to the methionine moiety of SAM. Motifs II and III are less conserved, with motif II containing a negatively charged amino acid that interacts with the ribose hydroxyls of SAM and a bulky hydrophobic side chain that makes contact with the adenine residue of SAM (Fig. 2). Motif III contains a conserved residue that interacts directly with the exocyclic amino group of the target adenine residue. Motif IV contains a string of highly conserved amino acid residues and creates a structure known as the P loop, which, along with motifs VI and VIII, forms the active or catalytic site of the enzyme. Motif V contains a conserved consensus sequence that contacts the SAM adenine residue and interacts with motif VII to form the SAM-binding site. Motif VI consists of a cluster of three hydrophobic residues that have been suggested to be involved in placement of the target adenine ring opposite motif IV. Motif VII is not strongly conserved but is believed to be involved in the folding of the catalytic region (5). Motif VIII is highly conserved and contains a phenylalanine residue that is also proposed to interact with the target adenine residue. This region forms a loop that hangs over the active site and is referred to as the "adenine-binding loop" (4). Motif X is not well conserved; however, in all methyltransferases the loop formed by motif X, along with the G loop of motif I and the P loop of motif IV, forms the sides of the binding pocket for the methionine moiety of SAM (21).

Motifs I, II, III, and X (Fig. 2) are primarily responsible for binding to SAM (6, 15, 16, 28) and have been collectively termed the SAM-binding region (21). Motifs IV, V, VI, VII, and VIII are primarily responsible for catalysis (28) as they form the active site and have been collectively termed the catalytic region (21). Methyltransferases belong to three groups that differ in the relative linear order of the SAM-binding region, the catalytic region, and the target recognition

* Corresponding author. Mailing address: Department of Microbiology, Monash University, Clayton, Victoria 3800, Australia. Phone: 61-3-9905-4825. Fax: 61-3-9905-4811. E-mail: Julian.Rood@med.monash.edu.au.

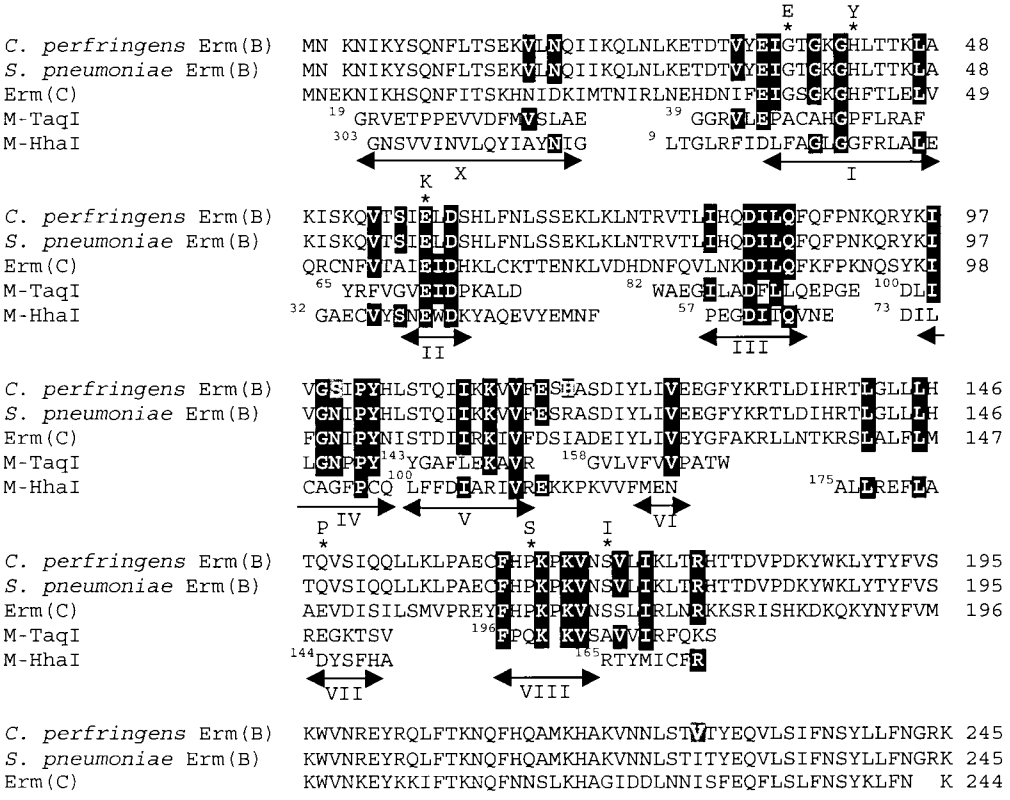

FIG. 1. Sequence alignment of DNA methyltransferases M-*Taq*I and M-*Hha*I and rRNA methyltransferases Erm(B) and Erm(C). The amino acid sequences of M-*Taq*I (GenBank accession no. JN0257) and M-*Hha*I (GenBank accession no. AAA24989) are aligned with the Erm(B) methyltransferases from *C. perfringens* (GenBank accession no. S16033) and *S. pneumoniae* (34) and the Erm(C) methyltransferase from *B. subtilis* (GenBank accession no. P13956). The position and extent of each of the conserved motifs, motifs I to VIII and X, are indicated by arrows below the sequence alignment. The superscript numbers to the left of the start of each M-*Taq*I or M-*Hha*I sequence indicates the starting residue number. Regions of identity between the DNA and rRNA methyltransferases are boxed in black. Amino acids in the *C. perfringens* Erm(B) sequence which differ from the *S. pneumoniae* Erm(B) amino acid sequence are boxed in grey. Amino acid mutations that were obtained in this study are indicated by an asterisk above the residue that was mutated and by the residue to which the amino acid was mutated. The figure was modified from reference 4.

region. Group α is arranged in the order (amino to carboxy) SAM-binding region, target recognition region, and catalytic region. Group β is arranged in the order catalytic region, target recognition region, and SAM-binding region. Group γ is arranged in the order SAM-binding region, catalytic region, and target recognition region (21).

The Erm(B) MLS or erythromycin resistance protein from the anaerobic pathogen *Clostridium perfringens* is a 23S rRNA methyltransferase that, on the basis of its amino acid sequence and the linear order of the conserved motifs, belongs to the γ group of methyltransferases (Fig. 1) (21). In this study we present the results of a random mutational analysis of the *C. perfringens erm*(B) gene and identify several amino acid residues located in conserved motifs that are important for either the structure or the function of the Erm(B) protein.

MATERIALS AND METHODS

Strains and media. The bacterial strains and plasmids used in the study are listed in Table 1. *Escherichia coli* strains were grown in 2YT broth or agar (23), which was supplemented with 30 μg of chloramphenicol per ml or 150 μg of erythromycin per ml, when appropriate for plasmid selection. *C. perfringens* strains were grown in nutrient broth or on nutrient agar (NA) (25) supplemented with 5 μg of chloramphenicol per ml or 50 μg of erythromycin per ml, when appropriate for plasmid selection, in anaerobic jars (Oxoid) in an atmosphere of 80% N_2, 10% H_2, and 10% CO_2.

Hydroxylamine mutagenesis of pJIR418. Hydroxylamine mutagenesis was carried out essentially as described previously (12). Plasmid DNA was extracted from 500-ml *E. coli* cultures by a modified large-scale alkali lysis method (26) and was further purified by equilibrium centrifugation on cesium chloride-ethidium bromide density gradients. Samples of plasmid DNA (3 μg) were added to 5 volumes of 0.1 M sodium phosphate buffer (pH 6.0) containing 1 mM EDTA and 4 volumes of hydroxylamine hydrochloride (1 M, adjusted to pH 6.0 with NaOH). The mixtures were incubated at 70°C for 120 or 180 min, after which the reactions were terminated by direct ethanol precipitation. The treated DNA was phenol-chloroform extracted and was used to transform *E. coli* DH5α cells to chloramphenicol resistance (30 μg/ml). The resistant colonies were then patched onto 2YT agar plates containing either chloramphenicol (30 μg/ml) or erythromycin (150 μg/ml) to screen for derivatives of pJIR418 that no longer conferred erythromycin resistance.

Mutagenesis of pJIR418 by passage through XL1-Red. Random mutants with mutations in the *erm*(B) gene were isolated by passaging pJIR418 through the DNA repair-deficient strain XL1-Red (Stratagene), according to the specifications of the manufacturer. Three independently derived samples of pJIR418 DNA were isolated after passage through XL1-Red and were used to transform

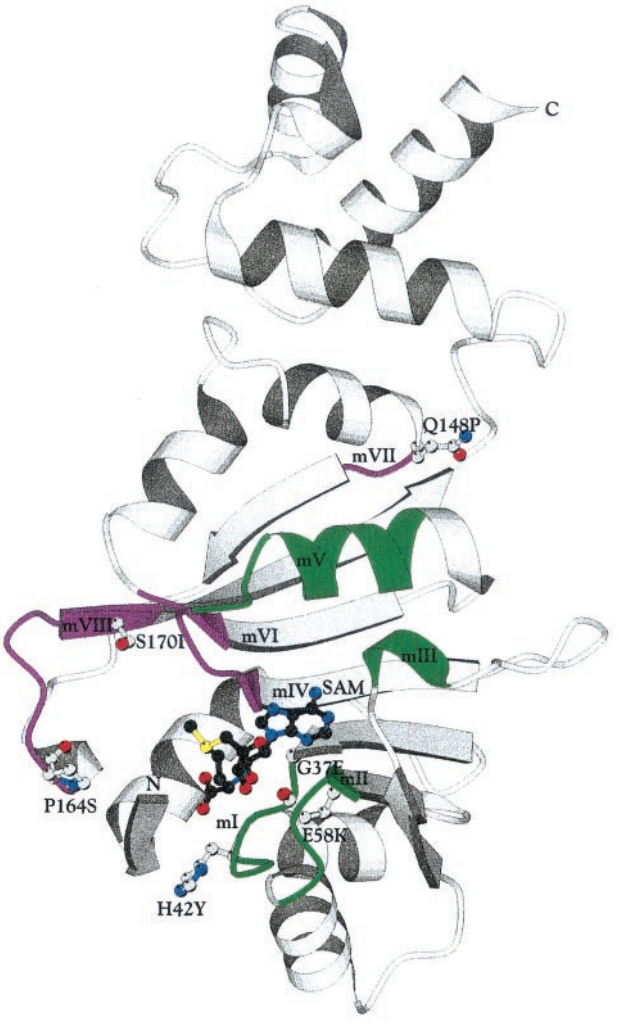

FIG. 2. Three-dimensional model of the Erm(B) protein from *C. perfringens*. The *C. perfringens* Erm(B) protein has a bilobate structure consisting of two domains. The upper (C-terminal) domain is the RNA-binding domain, which consists mainly of α helices. The lower (N-terminal) domain is the catalytic domain, which contains the putative SAM-binding region and the putative catalytic region. The locations of conserved motifs I to VIII (mI to mVIII) are shown in green and purple, and the positions of the residues mutated in this study are shown by indicating the side chain of the naturally occurring residue at these positions. The substrate, SAM, is shown in ball-and-stick fashion. The figure was drawn with the BOBSCRIPT program (7).

competent *E. coli* DH5α cells to chloramphenicol resistance (30 μg/ml), and erythromycin-sensitive derivatives were isolated as described above.

DNA sequence analysis. Plasmid DNA was extracted by a modified mini alkaline lysis-polyethylene glycol precipitation procedure (PRISM Ready Reaction Dye Deoxy Terminator Cycle Sequencing kit protocols; Applied Biosystems, Inc.). Sequencing of the mutated *erm*(B) genes was carried out with an ABI Prism Big Dye Terminator Cycle Sequencing Ready Reaction kit (Perkin-Elmer), as described by the manufacturer, with 3.2 pmol of primer per reaction mixture. Reactions were analyzed on an Applied Biosystems 373 DNA Sequencer. Sequence data obtained by automated sequencing were analyzed with Sequencher (version 3.0) computer software (Gene Codes Corp.).

Electroporation-mediated transformation of *C. perfringens*. Transformation of *C. perfringens* with pJIR418 or its derivatives was carried out by electroporation of lysostaphin-treated cells as described previously (30). Transformants were selected on NA containing 5 μg of chloramphenicol per ml.

Determination of erythromycin MICs. Erythromycin MICs were determined in both *E. coli* DH5α and *C. perfringens* JIR325 backgrounds essentially as described previously (14). *E. coli* strains were grown overnight in 20 ml of 2YT broth containing 30 μg of chloramphenicol per ml, while *C. perfringens* strains were grown overnight in 20 ml of brain heart infusion broth (Oxoid) containing 5 μg of chloramphenicol per ml. The overnight cultures were then diluted 1:25 in 10 ml of fresh 2YT or brain heart infusion broth containing 30 or 5 μg of chloramphenicol per ml, respectively, and were allowed to grow at 37°C until they reached a turbidity at 550 nm of 0.7 to 0.8. The cultures were then diluted 1:100 in fresh broth, and 10-μl aliquots were used to inoculate duplicate sets of either 2YT or NA plates, which contained either 30 or 5 μg of chloramphenicol per ml, respectively, and various concentrations of erythromycin. The cultures were incubated either aerobically (*E. coli*) or anaerobically (*C. perfringens*) for 18 to 24 h at 37°C. The MIC was recorded as the lowest concentration of erythromycin that completely inhibited growth.

Overexpression and purification of the Erm(B) protein. The *erm*(B) gene was amplified from pJIR418 by PCR with primers 6356 (5-GCGGGGGATCCATG AACAAAAATATAAAAT-3′) and 6357 (5′-CGCTTGGTACCTTATTTCCTC CCGTTA-3′), which introduce *Bam*HI and *Asp*718 sites immediately preceding the *erm*(B) start codon and immediately following the *erm*(B) stop codon, respectively. The 0.76-kb PCR product was digested with *Bam*HI and *Asp*718 and cloned into the expression vector pRSETA (Invitrogen Corp.). The resultant construct, pJIR1626, was sequenced to confirm that no base changes had occurred and was then introduced into *E. coli* expression strain BL21(DE3) (Stratagene). The His-tagged Erm(B) protein was purified from 1-liter cultures 3 h after induction with 2 mM isopropyl-β-D-thiogalactopyranoside by chromatography on Talon Metal Affinity Resin (Clontech). The Erm(B) protein was eluted from the column with 60 to 100 mM imidazole and was dialyzed against Tris-HCl buffer containing glycerol (50 mM Tris, 100 mM NaCl, 1 mM EDTA, 10% glycerol [pH 7.5]).

Production of Erm(B)-specific antisera. Purified His-Erm(B) protein was injected into female New Zealand White rabbits to elicit an immune response. The initial injection contained 50 μg of purified Erm(B) protein emulsified in Freund's complete adjuvant. Rabbits were boosted twice at 2-week intervals with 50 μg of purified His-Erm(B) protein emulsified in Freund's incomplete adjuvant and then bled via cardiac puncture. Prior to use in Western blot analyses, the Erm(B) antisera was adsorbed against cell extracts of BL21(DE3)(pRSETA) to remove nonspecific antibodies. The adsorbed antisera were used at dilutions of 1:5,000 in Western blot analyses.

Immunoblot analysis. Whole-cell lysates from *E. coli* strains harboring pJIR418 or one its derivatives were prepared from overnight cultures with a French press (RC-159; Applied Power Industry). The total protein concentration in each lysate was determined with a BCA protein assay kit (Pierce), according to the specifications of the manufacturer. Samples were prepared for electrophoresis by the addition of an equal volume of 2× sample buffer (100 mM Tris-HCl, 1% sodium dodecyl sulfate [SDS], 10% glycerol, 5% β-mercaptoethanol, 130 μg of bromophenol blue per ml [pH 6.8]), followed by boiling of the sample for 5 min. Standardized amounts of each lysate (10 μg) were loaded onto SDS–12% polyacrylamide gels alongside SeeBlue-prestained standards (Novel Experimental Technology). Electrophoresis was carried out in a Mini Protean II Electrophoresis Cell (Bio-Rad Laboratories) in Tris-glycine buffer (12.5 mM Tris-HCl, 100 mM glycine, 0.05% SDS) at 200 V until the dye front reached the bottom of the gel.

Western blotting was carried out essentially as described previously (32). Immediately following electrophoresis, the proteins were transferred to nitrocellulose (Schleicher & Schuell, Inc.) by electrophoresis in a mini Transblot Cell (Bio-Rad Laboratories) at 100 V for 1 h in Transblot buffer (12.5 mM Tris-HCl, 100 mM glycine, 10% methanol). Proteins were detected and visualized with Western blot Chemiluminescence Reagent (NEN Life Science Products), according to the specifications of the manufacturer.

Modeling of Erm(B) protein structure. The three-dimensional structure of Erm(B) was modeled on the crystal structure of ErmC′ in complex with the cofactor SAM (PDB entry 1QAO) (29). Initial modeling was performed with the program O (13) and then with Swiss Protein Data Bank Viewer software (http://www.expasy.ch/spdbv/) (9). The latter software provided the final energy-minimized model. Since Erm(B) and ErmC′ share approximately 50% sequence identity, a reliable model of Erm(B) was readily constructed without the need for any major adjustments.

RESULTS

Mutagenesis and isolation of *erm*(B) mutants. The *E. coli-C. perfringens* shuttle plasmid pJIR418 (31) carries two antibiotic resistance genes, the *erm*(B) gene and the *catP* gene, which

TABLE 1. Bacterial strains and plasmids

Strain	Relevant characteristics[a]	Source or reference
E. coli		
DH5α	F$^-$ ϕ80 d *lacZ*ΔM15Δ(*lacZYA-argF*)*U169 endA1 recA1 hadR17* (r_k^- m_k^-)*deoR thi-1 supE44 gyrA96 relA1*	Bethesda Research Laboratories
BL21(DE3)	F$^-$ *ompT hsd* S_B (r_B^- m_B^-) *gal dcm* (DE3)	Stratagene
XL1-Red	*endA1 gyrA96 thi-1 hsdR17 supE44 relA1 lac mutD5 mutS mutT* Tn*10* (Tc^r)	Stratagene
C. perfringens JIR325	Rif^r Nal^r derivative of strain 13	20
Plasmids		
pJIR418	*E. coli-C. perfringens* shuttle vector, Em^r Cm^r	31
pJIR750	pJIR418Δ[*Ava*II Klenow-*Sca*I *erm*(B)], *E. coli-C. perfringens* shuttle vector, Em^s Cm^r	2
pJIR1626	pRSETA(*Bam*HI-*Asp*718)Ω(0.76-kb product) from pJIR418 by PCR with primers 6356 and 6357), 3.7 kb, Em^r Ap^r	Recombinant
pRSETA	pUC-derived expression vector, N-terminal six-His tag, Ap^r	Invitrogen

[a] Em, Cm, Tc, Ap, Nal, and Rif, erythromycin, chloramphenicol, tetracycline, ampicillin, nalidixic acid, and rifampin, respectively.

confers chloramphenicol resistance. Therefore, it is ideal for use in mutagenesis because chloramphenicol-resistant transformants can be selected and then screened for erythromycin susceptibility. Two different mutagenesis techniques were used: in vitro mutagenesis of purified pJIR418 DNA with hydroxylamine and in vivo mutagenesis by passage through the mutator strain XL1-Red. After mutagenesis the mutated plasmid DNA was used to transform *E. coli* DH5α to chloramphenicol resistance, and the resultant colonies were patched onto NA containing either chloramphenicol or erythromycin. Colonies that grew on chloramphenicol but not on erythromycin were selected as those that contained potential *erm*(B) mutations. Over 9,000 chloramphenicol-resistant colonies resulting from three independent hydroxylamine mutagenesis reactions and three independent XL1-Red mutagenesis reactions were screened in this manner, leading to the isolation of 38 chloramphenicol-resistant, erythromycin-sensitive colonies. Restriction endonuclease analysis showed that 30 of these mutants had a normal pJIR418 profile (data not shown).

Sequence analysis of *erm*(B) mutants. Both strands of the potential *erm*(B) mutants were sequenced to identify their precise mutations. Two categories of erythromycin-sensitive mutants were identified. Nine of the mutants were found to contain a single mutation in the *erm*(B) structural gene (Table 2). All of these mutations led to single amino acid changes that were scattered throughout the Erm(B) protein, but all occurred either within or within very close proximity to one of the conserved methyltransferase motifs (Fig. 1). Nineteen plasmids encoded truncated Erm(B) proteins that were derived from either the introduction of a stop codon or a frameshift mutation that resulted from the insertion or deletion of a single base (Table 3). The remaining plasmids were not studied further, as one contained multiple mutations and no mutation could be identified in the other.

Quantitative effect of mutations on erythromycin resistance. To examine the effect of each of the mutations on erythromycin resistance, we determined the erythromycin MICs for both *E. coli* and *C. perfringens* derivatives carrying the mutated pJIR418-derived plasmids. For the wild-type derivatives, DH5α(pJIR418) and JIR325(pJIR418), erythromycin MICs were >1,280 μg/ml for both host species, whereas for the respective negative controls the MICs were 160 and <5 μg/ml, respectively, in keeping with the inherent higher basal level of erythromycin resistance found in *E. coli*. The erythromycin MICs were between 80 and 640 μg/ml for each of the mutated plasmids in the *E. coli* background and <5 μg/ml in the *C. perfringens* background with the exception of pJIR1603, for which the MIC was 640 μg/ml in both species (Table 2). The plasmids that encoded truncated Erm(B) proteins were examined in a similar manner and were shown to confer little or no resistance to erythromycin, depending on the size of the resultant Erm(B) protein (Table 3).

To ensure that the point mutations in the *erm*(B) gene and not mutations elsewhere on pJIR418 were causing the erythromycin-sensitive phenotypes, the mutated *erm*(B) gene from each derivative was amplified by PCR and cloned into pJIR750 behind the *lac* promoter. The *erm*(B) genes in each of the pJIR750-derived recombinant plasmids was sequenced to ensure that no additional mutations had been introduced during PCR. Each of these plasmids was then used to transform *E. coli* DH5α, and the erythromycin MIC for each of the resultant derivatives was determined. All of the pJIR750-*erm*(B) mutant derivatives conferred an erythromycin-sensitive phenotype, indicating that the mutation in the *erm*(B) gene was responsible for the erythromycin-sensitive phenotype (data not shown).

TABLE 2. Characteristics of erythromycin-sensitive Erm(B) derivatives containing missense mutations

Plasmid(s)	*erm*(B) nucleotide change[a]	Erm(B) amino acid change[b]	Erythromycin MIC (μg/ml)	
			E. coli	*C. perfringens*
pJIR418	NA	Wild type	>1,280	>1280
pJIR750	NA	Negative control	160	<5
pJIR1576	G1620A	G37E	160	<5
pJIR1615	C1634T	H42Y	160	<5
pJIR883	G1682A	E58K	80	<5
pJIR1603	T1698C	L63P	640	640
pJIR1606	A1953C	Q148P	320	<5
pJIR977, pJIR934, pJIR1571	C2000T	P164S	640	<5
pJIR1613	G2019T	S170I	640	<5

[a] Nucleotide positions refer to the previously published sequence of the *erm*(B) gene region from *C. perfringens* (3) (GenBank accession no. U18931). Nucleotide position 1511 is the first base of the *erm*(B) structural gene. NA, not applicable.

[b] The designations indicate the original Erm(B) residue, number of the residue, mutant residue.

TABLE 3. Characteristics of erythromycin-sensitive Erm(B) truncation derivatives

Plasmid(s)	*erm*(B) nucleotide change[a]	Erm(B) amino acid change[b]	Erm(B) size (no. of amino acids)	Erythromycin MIC (μg/ml)	
				E. coli	*C. perfringens*
pJIR418	NA	Wild type	245	>1,280	>1,280
pJIR750	NA	Negative control		160	<5
pJIR1599	26ΔA	Erm(B)8 + 3*	11	160	<5
pJIR1596, pJIR1598, pJIR1605	44ΔA	Erm(B)14 + 6*	20	160	<5
pJIR932, pJIR1570, pJIR1611	C1772T	Erm(B)88*	88	80	<5
pJIR1607	1841+A	Erm(B)110 + 5*	115	640	<5
pJIR1595, pJIR1597, pJIR1600	1851+T	Erm(B)113 + 2*	115	160	<5
pJIR1604	1851ΔT	Erm(B)113 + 10*	123	160	<5
pJIR971, pJIR973, pJIR1551	C1925T	Erm(B)139*	139	320, 320, 160	<5, 10, <5
pJIR1602	C1951T	Erm(B)148*	148	160	<5
pJIR1608, pJIR1609	C2120T	Erm(B)204*	204	160, 320	<5, <5
pJIR1610, pJIR1614	C2198T	Erm(B)230*	230	320	<5

[a] Nucleotide positions refer to the previously published sequence of the *erm*(B) gene region from *C. perfringens* (3) (GenBank accession no. U18931). Nucleotide position 1511 is the first base of the *erm*(B) structural gene. NA, not applicable.

[b] Mutations have introduced either stop codons (*), e.g., Erm(B)88*, or a frame shift which leads to a certain number of normal Erm(B)-encoded residues plus the indicated number of new amino acid residues following the frame shift up to the next stop codon, e.g., Erm(B)8 + 3*.

Detection of mutant proteins by immunoblotting. To examine the level of expression of the mutant Erm(B) proteins, whole-cell lysates were prepared from six of the DH5α derivatives carrying plasmids that encoded point mutations. Immunoblotting was carried out with an Erm(B)-specific polyclonal antiserum that was raised by use of purified Erm(B) protein expressed from the pRSETA expression vector construct, pJIR1626 (Table 1). All six of the mutants produced similar levels of a protein of the same size as the wild-type protein (Fig. 3), indicating that the erythromycin-sensitive phenotype exhibited by these mutants was due to a difference in the structure or function of the Erm(B) protein rather than poor expression or decreased stability of the protein.

Structural modeling of Erm(B) derivatives. The crystal structure of the rRNA methyltransferase ErmC′ from *Bacillus subtilis* (4, 29) and the nuclear magnetic resonance structure of the closely related rRNA methyltransferase Erm(B) (previously known as ErmAM [24]) from *Streptococcus pneumoniae* (34) have been determined. The streptococcal Erm(B) protein is nearly identical to the Erm(B) protein from *C. perfringens*, differing in only three amino acid residues, at positions 100, 118, and 226 (Fig. 1). On the basis of the crystal structure of Erm(C) (PDB entry 1QAO), a structure of the *C. perfringens* Erm(B) protein was constructed (Fig. 2). The model is bilobal, being folded in two main domains. The N-terminal domain is the catalytic domain that contains the SAM-binding region and the catalytic region, and the C-terminal domain is the RNA-binding domain. Based on this model, as in all other methyltransferases, motifs I to VIII and X form the basis of the SAM-binding region and the catalytic region.

Each of the six point mutations that we obtained in the *erm*(B) gene results in a change to an amino acid located either within or close to a conserved motif within this structure (Fig. 1). We obtained two mutations within or close to motif I (G37E and H42Y), one mutation in motif II (E58K), one mutation in motif VII (Q148P), and two mutations in or close to motif VIII (P164S and S170I). In an attempt to determine the effect of each of these mutations on the structure and function of the Erm(B) protein, we repeated the modeling process, but this time we incorporated the mutated residue into the amino acid sequence. The structures produced from this modeling are shown in Fig. 4 and Fig. 5. In each instance the mutation has affected the structure of the Erm(B) protein in or around either the SAM-binding region or the catalytic region and therefore is likely to affect either SAM binding or catalytic activity.

DISCUSSION

Treatment of bacterial infections with MLS antibiotics is often compromised by the presence of resistance determinants that encode Erm rRNA methyltransferases (35). The development of specific inhibitors of these enzymes is therefore of potential clinical significance. An important step in this process involves the determination of which motifs and residues of these proteins are critical for their function.

In this study we have used two separate random mutagenesis techniques to obtain 28 mutants that produced nonfunctional Erm(B) proteins. Eight of these mutants had single amino acid changes that abolished MLS resistance in both the *C. perfringens* and the *E. coli* backgrounds. These mutants contained point mutations at six distinct sites, each of which occurred within or close to conserved methyltransferase motifs that are

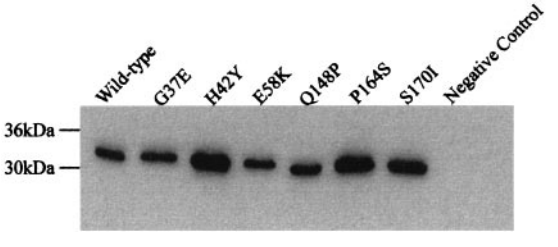

FIG. 3. Immunoblot analysis of mutant proteins. Standardized amounts (10 μg) of whole-cell lysates prepared from *E. coli* strains producing the indicated Erm(B) derivatives were separated by electrophoresis on a 12% polyacrylamide gel and transferred onto nitrocellulose with a Transblot Cell. The Erm(B) derivatives were detected with Erm(B)-specific polyclonal antiserum. The wild-type Erm(B) protein was detected in a whole-cell lysate from *E. coli* DH5α(pJIR418), and the negative control was a whole-cell lysate from *E. coli* DH5α(pJIR750).

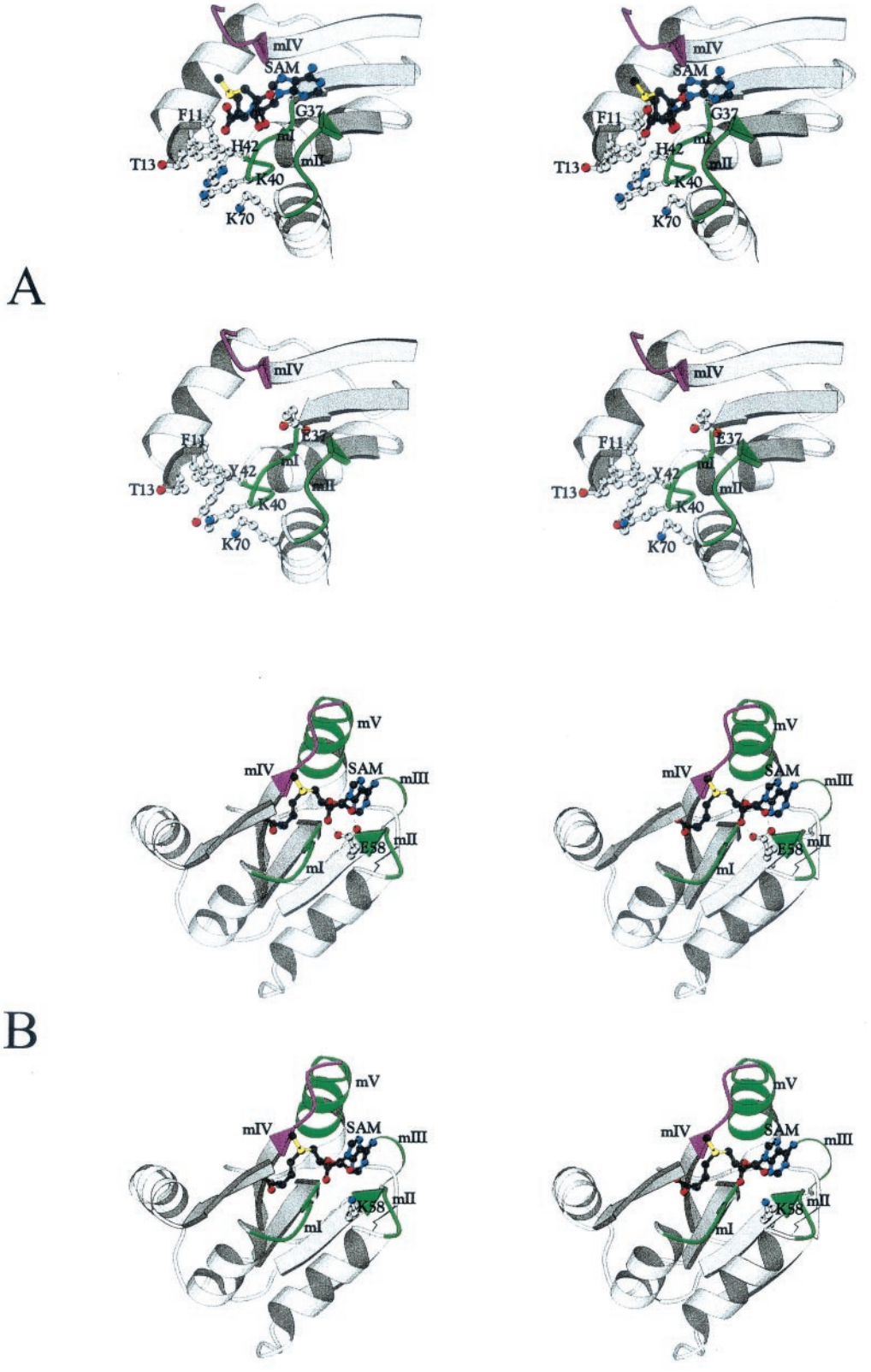

FIG. 4. Stereo views of the environment around each mutation in motifs I and II. Key residues are shown in ball-and-stick fashion. The top pair in each panel is a stereo view of the wild-type structure, and the lower pair in each panel shows the mutation. (A) Motif I mutations (G37E and H42Y). (B) Motif II mutation (E58K). mI to mV, motifs I to V, respectively. These figures were produced with the BOBSCRIPT program (7).

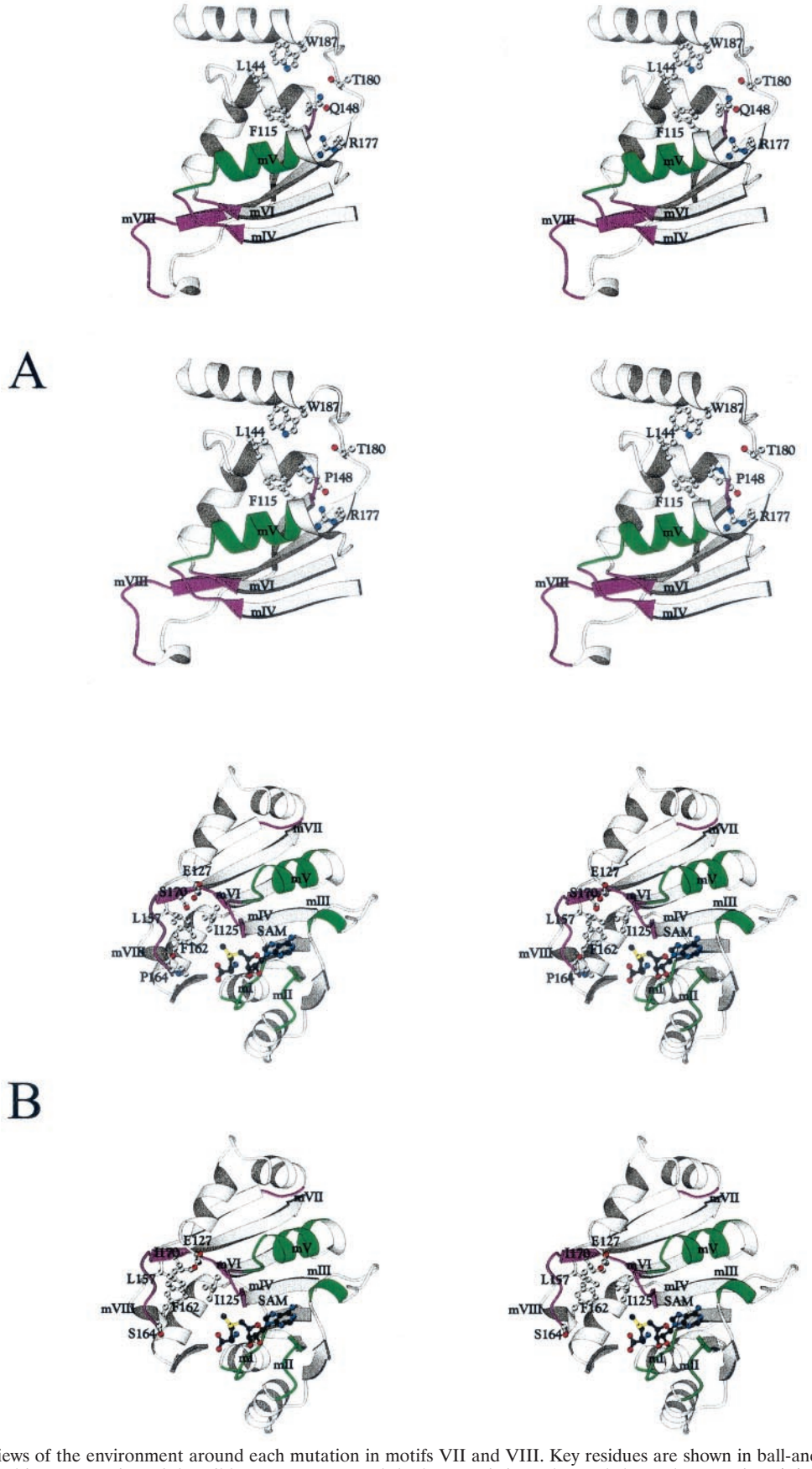

FIG. 5. Stereo views of the environment around each mutation in motifs VII and VIII. Key residues are shown in ball-and-stick fashion. The top pair in each panel is a stereo view of the wild-type structure, and the lower pair in each panel shows the mutation. (A) Motif VII mutation (Q148P). (B) Motif VIII mutations (S70I and P164S). mI to mVIII, motifs I to VIII, respectively. These figures were produced with the BOBSCRIPT program (7).

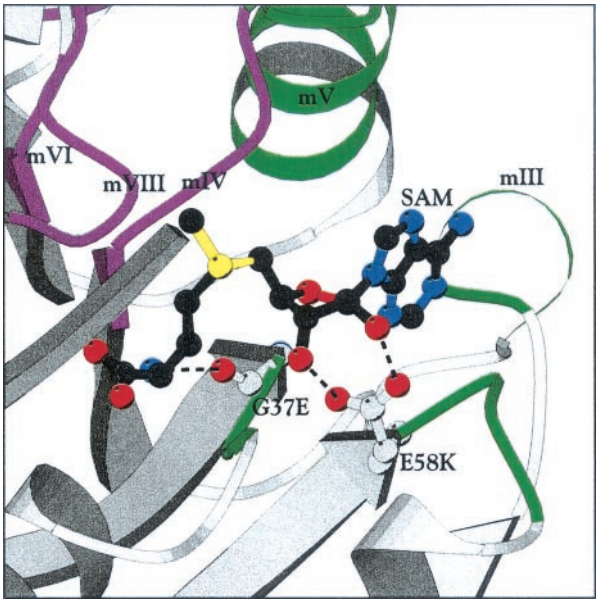

FIG. 6. Interactions between SAM and residues in motifs I and II. The model of the Erm(B) protein in the region surrounding the SAM molecule is shown. The locations of conserved motifs I to VI and VIII are shown in green and purple. The interactions between the glycine residue in motif I and SAM and the glutamate residue in motif II and SAM are indicated by dashed lines between the side chain of the residue and the SAM molecule. mIII, mIV, mV, and mVI, motifs III, IV, V, and VI, respectively. The figure was drawn with the BOBSCRIPT program (7).

involved either in SAM binding or in catalysis of the methylation reaction.

Methyltransferase motif I creates part of the binding pocket for the methionine and ribose regions of SAM (Fig. 6). The motif is centered around glycine-X-glycine residues (Fig. 1) and is typically preceded by an aspartate or a glutamate residue four amino acids closer to the N terminus (4). It forms a secondary structure known as the G loop, which binds to the methionine moiety of SAM (21). G37 and H42 are located within motif I. Upon binding of SAM, a change in the backbone conformation of G37 allows the main-chain carbonyl oxygen of this residue to accept a hydrogen bond from the α-amino nitrogen of SAM (29). This reaction implies that structural flexibility is very important at this particular residue. In addition, the torsion angles of G37 lie in the area of the left-handed helix region of the Ramachandran plot, which suggests that other amino acids will not be readily tolerated in this conformation. Therefore, the mutant that we obtained, G37E, is unlikely to be able to bind to SAM either due to the lack of flexibility in motif I or due to the steric hindrance of the glutamate side chain partially occupying the methionine portion of the SAM-binding site (Fig. 4A). The second mutant that we obtained in motif I, H42Y, is not as easily explained as G37E. The mutation occurs in a histidine residue that is not well conserved among methyltransferases. The *C. perfringens* Erm(B) model (Fig. 2) predicts that H42 would be exposed and that its mutation to tyrosine could easily be accommodated in the model without significant alterations to the structure (Fig. 4A). However, structurally, H42 is in the vicinity of both motif VIII and the SAM-binding site and may influence the binding of the RNA substrate either directly or indirectly through long-distance structural changes.

Motif II, like motif I, forms part of the SAM-binding pocket. This motif contains a negatively charged residue that forms a hydrogen bond with the ribose hydroxyls of SAM and is followed by a hydrophobic residue, which is in contact with the adenine ring of SAM through van der Waals forces (4). In the *C. perfringens* Erm(B) protein, E58 is the negatively charged residue and L59 is the hydrophobic residue (Fig. 1). Mutation of E58 to lysine, which is positively charged, should therefore also interfere with SAM binding (Fig. 4B). Note that another amino acid change, L63P, was also obtained in this region. This mutation had less significant effects on erythromycin resistance.

Motif VII is weakly conserved among methyltransferases; however, credible candidates can be found in most proteins (21). This motif is believed to play a role in the folding of the catalytic region (5). In this study we obtained a mutant in which the motif VII Q148 residue was changed to proline (Fig. 5A). This change does not cause any steric clashes in the structure; however, since motif VII is proposed to play a role in folding of the catalytic region, mutation of the glutamine residue to proline may influence RNA binding because of changes in the folding of the catalytic site.

Motif VIII is believed to be involved in the recognition of the adenine residue in the target RNA. It contains a phenylalanine residue that has been proposed to interact with the target adenine (28) and to play a role in catalysis via cation-π orbital interactions (27). This motif occurs in the adenine-binding loop, which forms a prominent arched feature over the catalytic domain (4) and which comprises the residues 162-FHPKPKVNS-170 in the *C. perfringens* Erm(B) protein. The motif is very well conserved among methyltransferase proteins and appears to have the consensus sequence of FXPXPXVXS (4). The first proline residue in this sequence is one of the key residues in the adenine-binding loop. This proline residue is conserved in Erm methyltransferases and is unambiguously found in the *cis* conformation (29), which is important for the conformation of the adenine-binding loop. In this study we obtained two mutations in motif VIII, P164S and S170I. Mutation of the key proline residue of this motif, P164, to serine would alter the conformation of motif VIII (Fig. 5B) and would therefore disrupt RNA binding. By contrast, the S170I mutation is probably the most difficult mutation to explain. On the basis of the predicted structure of the *C. perfringens* Erm(B) protein, there are two possible explanations that would account for the loss of erythromycin resistance. First, S170 is in contact with the conserved phenylalanine residue, which is predicted to be involved in the correct positioning of the target adenine. Therefore, the S170I mutation could perturb adenine binding due to subtle changes in the binding pocket, which in turn would probably be sufficient to prevent transfer of the methyl group from SAM to the target. Second, S170 may form a hydrogen bond with E127, which in turn may interact with Y103, the conserved tyrosine residue in the catalytic sequence formed by motif IV. The S170I mutation may therefore destabilize the structure in the catalytic region and result in these mutants being unable to catalyze the transfer of the methyl group from SAM to the RNA target.

Recent studies have reported on several potential Erm in-

hibitors whose actions are based on the ability of the end product of the methylation reaction, *S*-adenosyl-L-homocysteine, to inhibit the methylation reaction (10, 11). These potential inhibitors bind to the active site of the Erm protein, thereby competing with the substrate of the methylation reaction, SAM. In this study we have identified several regions other than the active or catalytic site of the protein and have shown that these regions are also critical for the function of the Erm(B) methyltransferase. These residues and motifs are generally well conserved among the Erm proteins and may represent potential targets for the development of inhibitors of this family of enzymes. Note that the application of combinatorial phage display technology has led to the discovery of several short peptides that bind to the ErmC protein and inhibit its activity (8). This type of approach provides an alternative method for the identification of Erm inhibitors.

ACKNOWLEDGMENTS

This project was supported by research grants to J.I.R. from the Australian National Health and Medical Research Council. K.A.F. was the recipient of an Australian Postgraduate Award. M.W.P. is an Australian Research Council Senior Research Fellow

REFERENCES

1. **Andersson, S., and C. G. Kurland.** 1987. Elongating ribosomes *in vivo* are refractory to erythromycin. Biochimie **69:**901–904.
2. **Bannam, T. L., and J. I. Rood.** 1993. *Clostridium perfringens-Escherichia coli* shuttle vectors that carry single antibiotic resistance determinants. Plasmid **229:**233–235.
3. **Berryman, D. I., and J. I. Rood.** 1995. The closely related *ermB-ermAM* genes from *Clostridium perfringens*, *Enterococcus faecalis* (pAMβ1), and *Streptococcus agalactiae* (pIP501) are flanked by variants of a directly repeated sequence. Antimicrob. Agents Chemother. **39:**1830–1834.
4. **Bussiere, D. E., S. W. Muchmore, C. G. Dealwis, G. Schluckebier, V. L. Nienaber, R. P. Edalji, K. A. Walter, U. S. Ladror, T. F. Holzman, and C. Abad-Zapatero.** 1998. Crystal structure of ErmC′, an rRNA methyltransferase which mediates antibiotic resistance in bacteria. Biochemistry **37:** 7103–7112.
5. **Cheng, X.** 1995. Structure and function of DNA methyltransferases. Annu. Rev. Biophys. Biomol. Struct. **24:**293–318.
6. **Cheng, X., S. Kumar, J. Pósfai, J. W. Pflugrath, and R. J. Roberts.** 1993. Crystal structure of the *Hha*I DNA methyltransferase complexed with *S*-adenosyl-L-methionine. Cell **74:**299–307.
7. **Esnouf, R. M.** 1999. Further additions to MolScript version 1.4, including reading and contouring of electron-density maps. Acta Crystallogr. D Biol. Crystallogr. **55:**938–940.
8. **Giannattasio, R. B., and B. Weisblum.** 2000. Modulation of Erm methyltransferase activity by peptides derived from phage display. Antimicrob. Agents Chemother. **44:**1961–1963.
9. **Guex, N., and M. C. Peitsch.** 1997. SWISS-MODEL and the Swiss-Pdb Viewer. An environment for comparative protein modeling. Electrophoresis **18:**2714–2723.
10. **Hajduk, P. J., J. Dinges, J. M. Schkeryantz, D. Janowick, M. Kaminski, M. Tufano, D. J. Augeri, A. Petros, V. L. Nienaber, P. Zhong, R. Hammond, M. Coen, B. Beutel, L. Katz, and S. W. Fesik.** 1999. Novel inhibitors of Erm methyltransferases from NMR and parallel synthesis. J. Med. Chem. **42:** 3852–3859.
11. **Hanessian, S., and P. W. M. Sgarbi.** 2000. Design and synthesis of mimics of *S*-adenosyl-L-homocysteine as potential inhibitors of erythromycin methyltransferases. Bioorg. Med. Chem. Lett. **10:**433–437.
12. **Humphreys, G. O., G. A. Willshaw, H. R. Smith, and E. S. Anderson.** 1976. Mutagenesis of plasmid DNA with hydroxylamine: isolation of mutants of multi-copy plasmids. Mol. Gen. Genet. **145:**101–108.
13. **Jones, T. A., S. Cowan, J. Y. Zou, and M. Kjeldgaard.** 1991. Improved methods for building protein models in electron density maps and the location of errors in these models. Acta Crystallogr. A **47:**110–119.
14. **Kennan, R. M., L. M. McMurray, S. B. Levy, and J. I. Rood.** 1997. Glutamate residues located within putative transmembrane helices are essential for TetA(P)-mediated tetracycline efflux. J. Bacteriol. **179:**7011–7015.
15. **Klimasauskas, S., S. Kumar, R. J. Roberts, and X. Cheng.** 1994. *Hha*I methyltransferase flips its target base out of the DNA helix. Cell **76:**357–369.
16. **Labahn, J., J. Granzin, G. Schluckebier, D. P. Robinson, W. E. Jack, I. Schildkraut, and W. Saenger.** 1994. Three-dimensional structure of the adenine specific DNA methyltransferase M. *Taq*I in complex with the cofactor *S*-adenosylmethionine. Proc. Natl. Acad. Sci. USA **91:**10957–10961.
17. **Lai, C. J., and B. Weisblum.** 1971. Altered methylation of ribosomal RNA in an erythromycin-resistant strain of *Staphylococcus aureus*. Proc. Natl. Acad. Sci. USA **68:**856–860.
18. **Leclercq, R., and P. Courvalin.** 1991. Bacterial resistance to macrolide, lincosamide, and streptogramin antibiotics by target modification. Antimicrob. Agents Chemother. **35:**1267–1272.
19. **Leclercq, R., and P. Courvalin.** 1991. Intrinsic and unusual resistance to macrolide, lincosamide, and streptogramin antibiotics in bacteria. Antimicrob. Agents Chemother. **35:**1273–1276.
20. **Lyristis, M., A. E. Bryant, J. Sloan, M. M. Awad, I. T. Nisbet, D. L. Stevens, and J. I. Rood.** 1994. Identification and molecular analysis of a locus that regulates extracellular toxin production in *Clostridium perfringens*. Mol. Microbiol. **12:**761–777.
21. **Malone, T., R. M. Blumenthal, and X. Cheng.** 1995. Structure-guided analysis reveals nine sequence motifs conserved among DNA amino-methyltransferases, and suggests a catalytic mechanism for these enzymes. J. Mol. Biol. **253:**618–632.
22. **Menninger, J. R.** 1995. Mechanism of inhibition of protein synthesis by macrolide and lincosamide antibiotics. J. Basic Clin. Physiol. Pharmacol. **6:**229–250.
23. **Miller, J. H.** 1972. Experiments in molecular genetics. Cold Spring Harbor Laboratory Press, Cold Spring Harbor, N.Y.
24. **Roberts, M. C., J. Sutcliffe, P. Courvalin, L. B. Jensen, J. I. Rood, and H. Seppala.** 1999. Nomenclature for macrolide and macrolide-lincosamide-streptogramin B antibiotic resistance determinants. Antimicrob. Agents Chemother. **43:**2823–2830.
25. **Rood, J. I.** 1983. Transferable tetracycline resistance in *Clostridium perfringens* strains of porcine origin. Can. J. Microbiol. **29:**1241–1246.
26. **Sambrook, J., E. F. Fritsch, and T. Maniatis.** 1989. Molecular cloning: a laboratory manual, 2nd ed. Cold Spring Harbor Laboratory Press, Cold Spring Harbor, N.Y.
27. **Schluckebier, G., J. Labahn, J. Granzin, and W. Saenger.** 1998. TaqI: possible catalysis via cation-pi interactions in N-specific DNA methyltransferases. Biol. Chem. **379:**389–400.
28. **Schluckebier, G., M. O'Gara, W. Saenger, and X. Cheng.** 1995. Universal catalytic domain structure of AdoMet-dependent methyltransferases. J. Mol. Biol. **247:**16–20.
29. **Schluckebier, G., P. Zhong, K. D. Stewart, T. J. Kavanaugh, and C. Abad-Zapatero.** 1999. The 2.2 Å structure of the rRNA methyltransferase ErmC′ and its complexes with cofactor and cofactor analogs: implications for the reaction mechanism. J. Mol. Biol. **289:**277–291.
30. **Scott, P. T., and J. I. Rood.** 1989. Electroporation-mediated transformation of lysostaphin-treated *Clostridium perfringens*. Gene **82:**327–333.
31. **Sloan, J., T. A. Warner, P. T. Scott, T. L. Bannam, D. I. Berryman, and J. I. Rood.** 1992. Construction of a sequenced *Clostridium perfringens-Escherichia coli* shuttle plasmid. Plasmid. **27:**207–219.
32. **Towbin, H., T. Staehelin, and J. Gordon.** 1979. Electrophoretic transfer of proteins from polyacrylamide gels to nitrocellulose sheets: procedure and some applications. Proc. Natl. Acad. Sci. USA **76:**4350–4354.
33. **Vester, B., and S. Douthwaite.** 2001. Macrolide resistance conferred by base substitutions in 23S rRNA. Antimicrob. Agents Chemother. **45:**1–12.
34. **Yu, L., A. M. Petros, A. Schnuchel, P. Zhong, J. M. Severin, K. Walter, T. F. Holzman, and S. W. Fesik.** 1997. Solution structure of an rRNA methyltransferase (ErmAM) that confers macrolide-lincosamide-streptogramin antibiotic resistance. Nat. Struct. Biol. **4:**483–489.
35. **Zhanel, G. G., and J. A. Karlowsky.** 1999. Ribosomal resistance: emerging problems and potential solutions. Curr. Infect. Dis. Rep. **1:**458–463.